

Application of the method of reducing rotating masses in mining transport systems

Marek MORAVIČ^{1*}, Daniela MARASOVÁ¹, Robert KRÓL², Maksymilian OZDOBA², Aleš SLÍVA³ and Dušan KUBALA¹

Authors' affiliations and addresses:

¹Faculty of Mining, Ecology, Process Control and Geotechnology, Technical University of Košice, Park Komenského 14, 042 00 Košice, Slovak Republic
e-mail: marek.moravic@tuke.sk
e-mail: daniela.marasova@tuke.sk
e-mail: dusan.kubala@tuke.sk

²Faculty of Geoenvironment, Mining and Geology Department of Mining, Wrocław University of Science and Technology, Na Grobli 15, 50-421 Wrocław, Poland
e-mail: robert.krol@pwr.edu.pl
e-mail: maksymilian.ozdoba@pwr.edu.pl

³Faculty of Mechanical Engineering, VSB – Technical University of Ostrava, 17. Listopadu 2172/15, 708 00 Ostrava, Czech Republic
e-mail: ales.sliva@vsb.cz

*Correspondence:

Marek Moravič, Faculty of Mining, Ecology, Process Control and Geotechnology, Technical University of Košice, Park Komenského 14, 042 00 Košice, Slovak Republic
tel.: +421 55 602 31 46
e-mail: marek.moravic@tuke.sk

Funding information:

This article was supported by the projects APVV-18-0248, APVV SK-PL-23-0052, VEGA 1/0728/24, KEGA 013TUKE-4/2023, SP2024/095, CZ.02.01.01/00/22_008/0004631, CZ.10.03.01/00/22_003/0000048

Acknowledgement:

This article was supported by the Slovak Research and Development Agency under the contract No. APVV-18-0248, APVV SK-PL-23-0052, VEGA 1/0728/24, KEGA 013TUKE-4/2023, by the project Students Grant Competition No. SP2024/095, by the State Budget of Czech Republic under Grant CZ.02.01.01/00/22_008/0004631 and in part by the EU through the REFRESH under project CZ.10.03.01/00/22_003/0000048.

How to cite this article:

Moravič, M., Marasová, D., Król, R., Ozdoba, M., Sliva, A. and Kubala, D. (2024). Application of the method of reducing rotating masses in mining transport systems. *Acta Montanistica Slovaca*, Volume 29 (4), 1058-1068

DOI:

<https://doi.org/10.46544/AMS.v29i4.22>

Abstract

In recent years, belt conveyors have been among the most widespread means of transport in the mining industry, and because of this, they are developing very quickly in terms of design. The key element of the belt conveyor is its drive unit. Random vibrations of the belt conveyor drive pose a great risk of downtime. The solution is to minimize dangerous vibrations occurring in the belt conveyor drive by predicting their occurrence using dynamic models. The article presents a complete dynamic model that describes the real mechanical system and its verification by the method of reducing the number of degrees of freedom of replacement dynamic torsion systems. When creating models, the method of partial frequencies is applied to a six-mass mechanical system. Subsequently, the calculation of the reduced new system is compared with the calculation of the original system. At the same time, a simulation calculation approach in the MATLAB program is also applied. The calculations aim to determine the specific angular frequencies and mode shapes for each degree of reduction and system type. The calculation model using the Holzer tabular method is verified by calculation in the MATLAB simulation program. Both approaches provide good technical accuracy with a tolerance of up to 5 %.

Keywords

Belt conveyor, natural frequency, mode shape, simulation, reduction, Holzer.



© 2024 by the authors. Submitted for possible open access publication under the terms and conditions of the Creative Commons Attribution (CC BY) license (<http://creativecommons.org/licenses/by/4.0/>).

Introduction

An efficient process of transporting raw materials by conveyor belt is possible only with the correct and undisturbed operation of conveyors and their components. Continuous monitoring of the conveyor is essential to ensure its safe operation. Conveyor belt transport represents an important transport system in a wide range of operations, especially in the extraction and processing of mineral resources. Important decisions in optimizing the operation of belt conveyors using the AHP method were described in the publication (Andreiova et al., 2015). In order to select suitable modifications to the design parameters of the belt conveyor, the drive was determined to be the most important structural element. The application of generally valid logistics principles when designing a conveyor belt logistics system can also increase the efficiency of the transport process. The authors' case study (Ambriško et al., 2015) presents the application of the general procedure of logistics system designing as a suitable method for deciding on possible changes in the examined belt conveyor system. During the transportation of raw materials belt conveyors, physical phenomena take place influenced by the vibrations of drums and rollers, which are considered mechanical oscillations with relatively low amplitude and relatively high frequency. Unexpected mechanical failures of the rotating masses of the belt conveyor during operation can lead to long downtime (Bortnowski et al., 2023), (Ambriško et al., 2023). Currently, thermal imaging is widely used as a simple approach to determine the operating state of a belt conveyor drive system design based on anomalies in thermographs (Szurgacz et al., 2021), (Dabek et al., 2022), (Pytlík and Trela, 2016). For the prevention of disorders, many methods for diagnosing disorders based on vibrational or vibroacoustic signals are described in the literature (Yu et al., 2022), (Jia et al., 2019), (Alharbi et al., 2023), (Nawrocki et al., 2023). Czech et al. (2014) examined diagnostics of damage to mechanical elements using vibration signals and artificial neural networks. Łazarz et al. (2011) used vibroacoustic problem-solving to detect gearbox component malfunctions. Likewise, the diagnosis of belt conveyor roller faults is mostly based on acoustic and vibration signals (Alhabri et al., 2023), (Li et al., 2013), concerns the use of vibration to detect roller faults, thermal methods present (Liu et al., 2020), and acoustic methods for detecting faults in belt conveyor systems (Wijaya et al., 2022), (Qurthobi et al., 2022). In a study by Zhang et al. (2023), mechanical faults of rollers were detected by a non-contact method of diagnosis using acoustic signals using MFCC (Mel-frequency Cepstral Coefficient) and weighted error detection SVDD (Support Vector Data Description) based on sample centre distance.

Alhabri et al. (2023) present an overview of fault detection using machine learning models based on acoustic and vibration signals for belt conveyors. Machine learning for vibration diagnostics was also applied by the authors Nowakowski et al. (2022). During the operation of belt conveyors, due to the large number of rotating masses, noise is also generated that spreads to the surroundings. Risk assessments depending on the sources of noise caused by conveyor systems were evaluated by Piňosová et al. (2018) and Thai et al. (2021). Many factors affect conveyor noise. The main noise sources of the belt conveyor include rotating masses such as roller bearings (Ladanyi, 2016). Added to this is the noise from the belt conveyor design, which is vibrated by the transmission of roller oscillations through their holders and also by the effect of material impact on the conveyor belt at the point of overflow (Ullmann et al., 1998), (Bortnowski et al., 2021). Upon impact of the material, the conveyor belt can be considered as a thin isotropic plate. Klimenda et al. (2022) derived the behaviour of thin isotropic plates under impact load and transverse wave propagation analytically in the MATLAB software environment. They compared the Kirchhoff and Rayleigh models in terms of shifts, speeds, and normal voltages. Another source of noise and vibration is the conveyor belt. An experimental study (Bortowski et al., 2022) demonstrated a significant effect of conveyor belt speed on noise and vibration emission. Noise emitted by machinery and equipment is also regulated by European Union directives (Directive 2000/14/EC) (Directive 2010/75/EU).

The process of continuous material feeding in conveyor belt is of great importance for both mining and processing industries (Zivanic et al., 2021). Fluctuations in material flow on the conveyor belt lead to harmful vibrations on both the belt and the conveyor. Zeng et al. (2020) proposed a dynamic model in terms of conveyor belt speed control during uneven transport of bulk material. They verified the model by using experimental measurements to analyze the mechanical behaviour of the belt. The research results confirmed the correctness of the models, and with the help of the proposed models, it is possible to optimize the operating procedures of belt conveyor systems. According to Ambrozkiewicz et al. (2021), one of the most common causes of vibration is the blockage of the rollers and, consequently, damage to the roller bearing. Current research is focused on expert fault diagnosis systems based on noise and vibration monitoring (Yang et al., 2020), (Skoczylas et al., 2021), (Bortowski et al., 2022).

For belt conveyors, transverse vibrations of a moving belt are particularly dangerous (Harrison, 1986). Frequent stopping and lowering of the conveyor adversely affect the service life of conveyor drive gearboxes, couplings, and bearings (Hou et al., 2008), (Pang and Lodewijks, 2013). Guohuan et al. (2011) describe the drive system of long belt conveyors with variable frequency and adjustable speed. In the research into the vibration of belt conveyors, the method of virtual prototyping is currently also used. The dynamic simulation of a belt conveyor based on virtual prototyping is presented in the publication by Guo et al. (2010). Likewise, Yan and He (2010) created a belt conveyor model and performed a dynamic analysis of it using virtual prototype technology. The

results of their research point to a new approach to analyzing the safety and structure of belt conveyors. Bortowski et al. (2022) proposed an LSTM neural network algorithm to automate the process of detecting anomalies of the recorded diagnostic signal based on a specified time series in identifying roller damage. This detection algorithm has been verified under both laboratory and in-situ conditions.

The appearance of vibrations on the belt conveyor can also be caused by misalignment of the location of the drive and return stations. Belt and structure vibrations can be caused by suboptimal drive operation due to the lack of soft-start devices, the drive unit's vibration, and the motors' non-synchronous operation (Damnjanović et al., 2017). Ojha et al. (2014), based on spectrum analysis and vibration measurements, found high axial and radial vibrations that were caused by a combination of parallel and angular misalignment between the engine and gearbox.

From the above overview of the current state of formation of vibrations and methods for measuring them in belt conveyors, it can be stated that various types of vibration sources contribute to the occurrence of vibrations in the structural parts of the belt conveyor, mainly imbalance of drums, misalignment, mechanical clearance of drum and roller bearings, resonance of the structure, excessive wear of roller bearings, etc.

In torsion-oscillating mechanical systems comprising flexible elements, dangerous torsional oscillations can be reduced to an acceptable extent by appropriate adaptation of dynamic properties (i.e., stiffness, damping, and moments of inertia) of these members of the system dynamics (Homišín and Moravič, 2016). Due to the inertial forces and variable torque of individual machines and equipment, dangerous torsional oscillations occur. Tuning of the mechanical system and avoidance of resonance by changing the stiffness value of a flexible element in the system was examined by Homišín and Moravič (2016). The results of vibration frequency measurements provide the information necessary for the correct operation of the conveyor. Distributed sensors can also be used to measure vibrations. Novotný et al. (2021) describe the application of a distributed remote sensing system using standard telecommunications single-mode optical fibre for distributed mechanical vibration sensing. According to Grega et al. (2018), torsional vibration reduction is possible by using new flexible coupling designs. Experiments verified the influence of pneumatic couplings filled with helium and propane-butane under laboratory conditions on the mechanical system.

This study proposes dynamic models for minimizing and partially eliminating vibrations to eliminate belt conveyor failures due to vibration and ensure its normal operation.

Materials and methods

Description of the mechanical system

The main structural parts of belt conveyors include the drive station, return station, tensioning station, support rollers, conveyor belt, and supplementary and protective devices. The drive station is one of the most important parts of the belt conveyor, as it ensures the movement of the conveyor belt. The classic belt conveyor drive station consists of separate structural parts: an electric motor, couplings, gearbox, and drive drum with bearings. All these components are mounted on a separate supporting frame (Fig. 1).

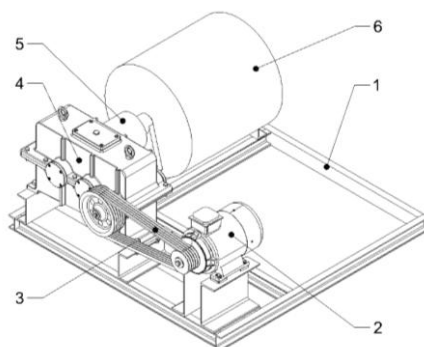


Fig. 1. The classic concept of a belt conveyor drive station:
1 – frame structure, 2 – electric motor, 3 – belt drive, 4 – gearbox, 5 – flexible coupling, 6 – drive drum.

The simplest power station is one power unit and a power drum. This configuration is sufficient for lightly loaded, short conveyors. Most conveyors have two, three, or four drive units and two drive drums. The task of belt conveyor drive is to transfer the power of the driving machine to one or more drive drums.

The mechanical system (Fig. 1) is driven by an asynchronous electric motor with torque-speed characteristic M_{AM} . At the output is a working appliance of power with load torque M_Z . Power from the electric motor is transmitted by belt drive through the gearbox to the drive drum shaft of the conveyor. The drive and driven part of the mechanical system is connected to a belt drive, a two-stage gearbox, and a flexible coupling. The coupling provides the transmission of load torque.

Theoretical basis of the partial frequency method

In order to calculate the dynamic properties of aggregates, it is necessary to replace the aggregate with an auxiliary system describing, to some extent, the actual system before compiling the equations of motion. From the experience of calculations of torsional oscillations of aggregates (Grega et al., 2019), it is possible to replace these aggregates with systems containing mass discs connected by intangible shafts. The masses of the cranks are considered constant. Also, the stiffness between individual masses is constant. Despite various steps of assumptions that things can be neglected, the substitute systems are quite complex. When calculating dynamic phenomena during the engine's starting or stopping, the calculation's main structure is the stress on the flexible couplings. Here, it is advisable to simplify the system so that the stresses on the couplings can be determined. When calculating at a steady state, it is necessary to perform the calculation on the complex system since the purpose of the calculation is to determine the stresses of the elements (crankshafts). Several methods for simplifying replacement torsion systems have been developed, such as the method of the centre of gravity of moments of inertia and the method of partial frequencies. According to Rivin (1966), the second method is designed to calculate lower natural frequencies and mode shapes of the torsion system with greater degrees of freedom. Simplification must be carried out in such a way that the error is as small as possible.

The partial frequencies method is a method of reducing complex systems to a simple reduced system (Utěkal, 1973), (Chen et al., 2020). This method is based on substituting subsystems consisting of two masses connected by a shaft or systems with one mass and two torsional stiffnesses (Rivin, 1966).

For each type of system α and β , a reduction to a maximum of a two-mass system is possible.

A mechanical system model with n -degrees of freedom can be converted into a system with $m < n$ degrees of freedom. For each partial system, calculate the partial natural angular frequency according to the relation (Utěkal, 1973):

$$\Omega^2 = \frac{k}{I} \tag{1}$$

Systems to which the following applies

$$\Omega^2 > \omega^2, \tag{2}$$

are converted into equivalent partial systems of the second type. These systems are then added to the core system.

We get a simplified system that has one degree of freedom, i.e., one less frequency of its own. This procedure can be repeated several times until a reduction in the number of masses to three or two is achieved. Once simplified, it becomes easier to calculate natural angular frequencies and mode shapes.

Calculation models

Mathematical model of a mechanical system

Dynamic analysis is used to assess the vibration rate in the system. When performing this dynamic analysis, the system is replaced by a mathematical model (Fig. 2), which consists of mass bodies connected by linear springs with stiffness k .

The principal representation of the torsion-oscillating mechanical system, specifically the belt conveyor drive, is shown in Fig. 2. Descriptions of individual quantities for Fig. 2 are given in Tab. 1.

The members of the system in Fig. 2, denoted as k , represent flexible terms, and I with indices are masses. The stiffness of the spur gears k_z teeth is very great relative to that of the coupling k_s , belt k_R , and conveyor belt k_p . After reducing it to a high-speed shaft and neglecting the flexibility of the gear teeth, we obtain a dynamic model according to Fig. 3, where the individual masses show the drive system of the belt conveyor.

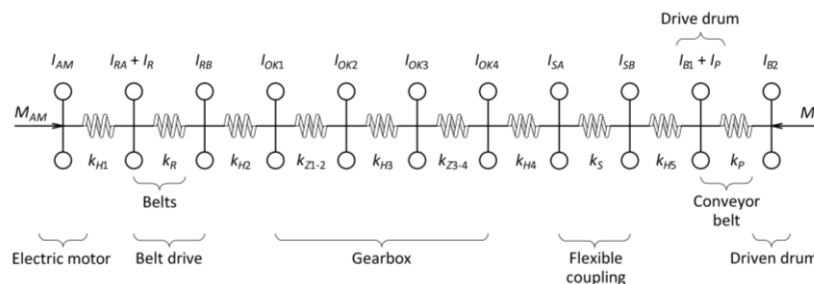


Fig. 2. Complete substitute for belt conveyor drive torsion system.

Tab. 1. Description of parameters for Fig. 2.

Parameter	Meaning
I_{AM}	Moment of inertia of electric motor (asynchronous motor)
I_{OK1}, \dots, I_{OK4}	Moment of inertia of individual gears in the gearbox
I_{RA}	Moment of inertia of a small pulley
I_{RB}	Moment of inertia of a large pulley
I_R	Moment of inertia of belts reduced to a small pulley
I_{SA}	Moment of inertia of the flexible coupling flange on the gearbox side
I_{SB}	Moment of inertia of the flexible coupling flange on the drive drum side
I_{B1}	Moment of inertia of the drive drum
I_{B2}	Moment of inertia of driven drum
I_P	Moment of inertia of the mass of material on the belt reduced to the drive drum
k_{H1}	Torsional stiffness of the shaft between I_{AM} and I_{RA}
k_{H2}	Torsional stiffness of the shaft between I_{RB} and I_{OK1}
k_{H3}	Torsional stiffness of the shaft between I_{OK2} and I_{OK3}
k_{H4}	Torsional stiffness of the shaft between I_{OK4} and I_{SA}
k_{H5}	Torsional stiffness of the shaft between I_{SB} and I_{B1}
k_R	Torsional belt stiffness
k_S	Torsional stiffness of the flexible coupling
k_P	Torsional stiffness of the conveyor belt
k_{Z1-2}, k_{Z3-4}	Stiffness of spur gear teeth
M_{AM}	Electric motor torque
M_Z	Load torque

The method is applied to a six-mass mechanical system (Fig. 3). In this case, the calculation performed is only a substitute for a system of type α for a system of type β . The input values are in Tab. 2 after the initial reduction to a high-speed shaft between rotating masses I_{AM} and $I_{RA} + I_R$.

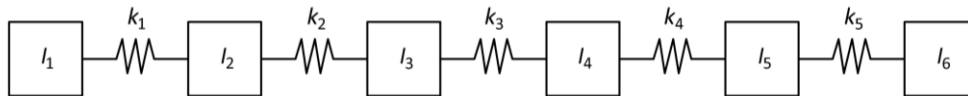


Fig. 3. Six-mass system.

Tab. 2. Moments of inertia and stiffness of the system.

i	I_i [kg·m ²]	k_i [N·m·rad ⁻¹]
1	0.04279	1604.020
2	0.05378	1060.240
3	0.00279	149.350
4	0.00048	16.674
5	0.05747	8.914
6	0.05734	—

Simulation model of the mechanical system

The dynamic model of the mechanical system in Fig. 3 is described by differential equations of motion that have been rewritten to the moment of inertia matrix I and the stiffness matrix k and entered as inputs to the MATLAB simulation program.

Fig. 4 describes the principle of operation of the algorithm used to calculate the quantities by the partial frequencies method in the MATLAB program.

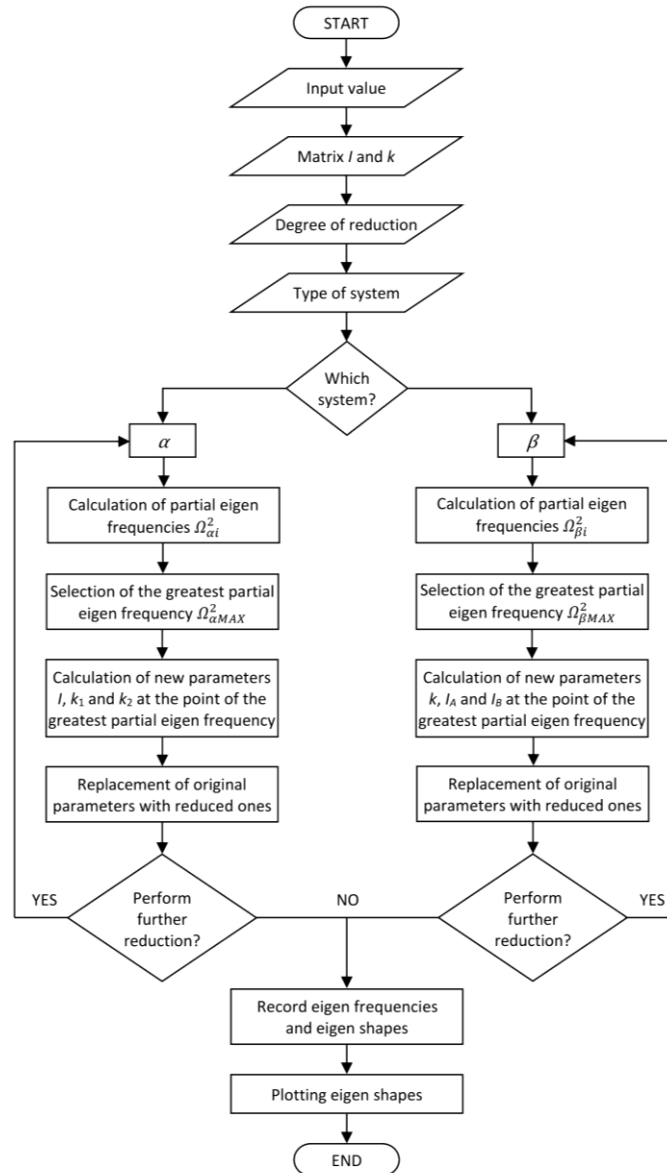


Fig. 4. Calculation algorithm in MATLAB.

Calculations and results

Calculation procedure

The calculation procedure is shown schematically in Fig. 5. First, we divide the system into type subsystems and calculate the natural angular frequencies according to the relation in Moravič (2017). Since the highest natural angular frequency has manifested itself in a system formed by discs I_2 and I_3 , we replace it with a system of type β using equations in Moravič (2017). We incorporate the new system into the original system to obtain a five-mass system. Repeating the above procedure, we obtain a two-mass system.

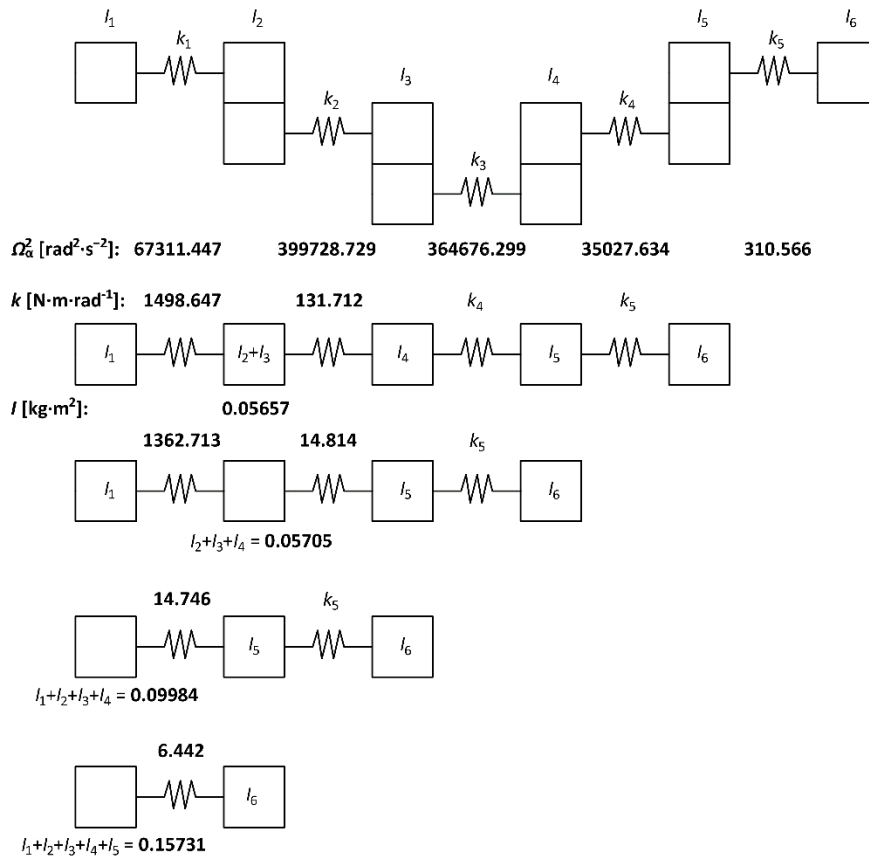


Fig. 5. Progressive simplification of the six-mass system to the two-mass system.

Calculation results

The results of the calculation of natural angular frequencies are shown in Tab. 3. The progressive simplification error is indicated by the symbol $\Delta\Omega_i$, expressed in %, and related to the natural angular frequency of the original six-mass system. The (+) sign in the column indicates an increase, and the (-) sign indicates the decrease of the new value of the natural angular frequency relative to the original.

Tab. 3. Calculated natural angular frequencies of a six-mass system with a gradual reduction to a set of two rotating masses of the belt conveyor (RMBC).

Number of RMBC	Ω_1 [rad·s $^{-1}$]	$\Delta\Omega_1$ [%]	Ω_2 [rad·s $^{-1}$]	$\Delta\Omega_2$ [%]	Ω_3 [rad·s $^{-1}$]	$\Delta\Omega_3$ [%]	Ω_4 [rad·s $^{-1}$]	$\Delta\Omega_4$ [%]	Ω_5 [rad·s $^{-1}$]	$\Delta\Omega_5$ [%]
6	12.36	0	23.73	0	255.68	0	514.34	0	732.41	0
5	12.36	0	23.73	0	247.31	-3.274	558.08	8.504	—	—
4	12.36	0	23.73	0	236.32	-7.572	—	—	—	—
3	12.35	-0.081	23.71	-0.084	—	—	—	—	—	—
2	12.38	0.162	—	—	—	—	—	—	—	—

Fig. 6 shows a graphical representation of the mode shape of the oscillation of the first natural angular frequency for the six-mass system and Fig. 7 for the second natural angular frequency. In Fig. 6 and Fig. 7, the amplitudes of masses are plotted on the vertical axis and the position of the individual masses on the horizontal axis. The position of the masses is characterized by their distance from each other, which represents the flexibility of the shafts. The values of the observed quantities given in Fig. 6 and Fig. 7 were calculated using the Holzer tabular method (Tab. 4 and Tab. 5).

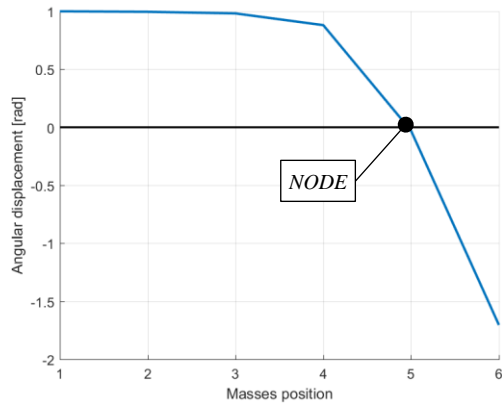


Fig. 6. Mode shapes of the 1st natural frequency for six-mass.

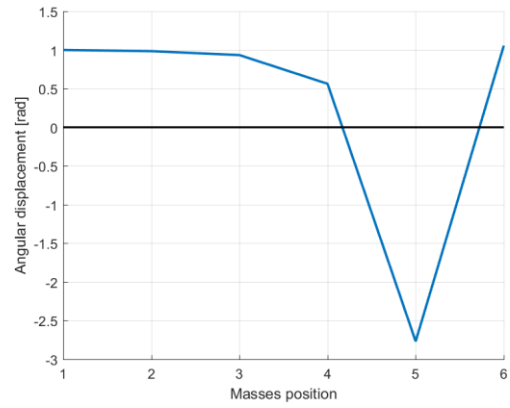


Fig. 7. Mode shapes of the 2nd natural frequency for six-mass.

Tab. 4. Mode shapes of single-node oscillation of the mechanical system.

$\Omega_1 = 12.35790 \text{ rad}\cdot\text{s}^{-1}, \Omega_1^2 = 152.71767 \text{ rad}^2\cdot\text{s}^{-2}$						
I	$I\cdot\Omega_1^2$	φ	$I\cdot\Omega_1^2\cdot\varphi$	$\sum I\cdot\Omega_1^2\cdot\varphi$	k	$\sum I\cdot\Omega_1^2\cdot\varphi/k$
0.04279	6.53479	1	6.53479	6.53479	1604.020	0.00407
0.05378	8.21316	0.99593	8.17970	14.71448	1060.240	0.01388
0.00279	0.42608	0.98205	0.41843	15.13292	149.350	0.10133
0.00048	0.07330	0.88072	0.06456	15.19748	16.674	0.91145
0.05747	8.77668	-0.03073	-0.26967	14.92781	8.914	1.67465
0.05734	8.75683	-1.70537	-14.93367	0	—	—

Tab. 5. Mode shapes of two-node oscillation of the mechanical system.

$\Omega_2 = 23.73000 \text{ rad}\cdot\text{s}^{-1}, \Omega_2^2 = 563.11290 \text{ rad}^2\cdot\text{s}^{-2}$						
I	$I\cdot\Omega_2^2$	φ	$I\cdot\Omega_2^2\cdot\varphi$	$\sum I\cdot\Omega_2^2\cdot\varphi$	k	$\sum I\cdot\Omega_2^2\cdot\varphi/k$
0.04279	24.09560	1	24.09560	24.09560	1604.020	0.01502
0.05378	30.28421	0.98498	29.82928	53.92488	1060.240	0.05086
0.00279	1.57108	0.93412	1.46758	55.39246	149.350	0.37089
0.00048	0.27029	0.56323	0.15224	55.54470	16.674	3.33122
0.05747	32.36210	-2.76799	-89.57794	-34.03325	8.914	-3.81795
0.05734	32.28889	1.04997	33.90222	0	—	—

Values of monitored quantities given in Tab. 6 were calculated using the MATLAB simulation program.

Tab. 6. Mode shapes of the six-mass mechanical system calculated in the MATLAB program.

	Ω_0	Ω_1	Ω_2	Ω_3	Ω_4	Ω_5
φ_1	1	1	1	1	1	1
φ_2	1	0.996	0.985	-0.744	-6.057	-13.31
φ_3	1	0.982	0.934	-0.915	64.544	327.204
φ_4	1	0.881	0.563	-1.015	246.776	-534.363
φ_5	1	-0.030	-2.77	0.004	-0.271	0.289
φ_6	1	-1.705	1.056	0	0	0

A node represents a point around which two masses oscillate. At this point, the angle of rotation has zero value, and the moment has maximum value.

The oscillating for the one-node (Fig. 6) mode shape of the six-mass system is between masses I_4 and I_5 . In the two-node (Fig. 7) mode shape, it is between the pair of masses $I_4 - I_5$ and $I_5 - I_6$. In the above case, there are constant distances between the masses. It is different in the case of comparison of two-mode shapes with different numbers of masses (Fig. 8). The actual distance of the position of each mass involves converting the stiffness k_i to the compliance c_i and multiplying by an appropriate scale.

Fig. 8 plots to scale the mode shape of the oscillation of the first natural angular frequency for the six-mass and the three-mass mechanical system. The position of the node of the six-mass and three-mass systems differs by 0.6 %, which can be neglected.

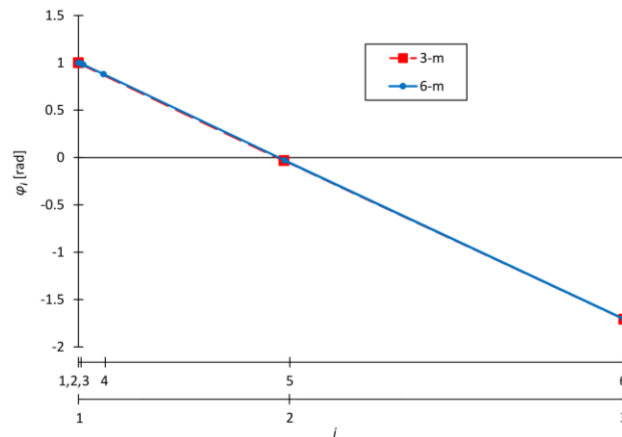


Fig. 8. Comparison of the one-node mode shape of the original and reduced mechanical system.

Discussion and conclusions

The calculation results show that the described method gives very good results not only for its natural angular frequencies (Tab. 3) but also for its mode shapes (Fig. 8), even when simplified to a two-mass system. It follows that the accuracy of the result using this method for technical practice is sufficient. Considering that the basic input data (moment of inertia and torsional stiffness) are also determined with a certain error, we can consider the accuracy of the result relevant.

The accuracy of the calculations is influenced by:

- error from the determination of input parameters, i.e., torsional stiffness of shafts and moments of inertia,
- the method used to determine the natural angular frequencies and the mode shapes of oscillations.

The proposed analytical method provides fast information already at the design stage of the mechanical system, unlike numerical virtual modelling methods where knowledge of the exact geometry is required to obtain relevant results.

The knowledge of excitation and natural frequencies contributes to the partial elimination of vibrations in mechanical systems.

References

- Alharbi, F., Luo, S., Zhang, H., Shaikat, K., Yang, G., Wheeler, C.A., Chen, Z. (2023). A Brief Review of Acoustic and Vibration Signal-Based Fault Detection for Belt Conveyor Idlers Using Machine Learning Models. *Sensors*, 23(4). <https://doi.org/10.3390/s23041902>
- Ambriško, L., Marasová, D. jr., Grendel, P., Lukáč, S. (2015). Application of logistics principles when designing the process of transportation of raw materials. *Acta Montanistica Slovaca*, 20(2),141-147.
- Ambriško, L., Marasová, D.jr., Klapko, P. (2023) Energy Balance of the Dynamic Impact Stressing of Conveyor Belts. *Appl. Sci.*, 13(7). <https://doi.org/10.3390/app13074104>
- Ambrozkiewicz, B., Syta, A., Meier, N., Litak, G., Georgiadis, A. (2021). Radial internal clearance analysis in ball bearings. *Eksploatacja i Niezawodność – Maintenance and Reliability*, 23(1), 42-54. <https://doi.org/10.17531/ein.2021.1.5>
- Andrejiová, M., Grinčová, A., Marasová, D., Grendel, P. (2015). Multicriterial assessment of the raw material transport. *Acta Montanistica Slovaca*, 20(1), 26-32. <https://doi.org/10.3390/ams20010026>
- Bortnowski, P., Doroszuk, B., Krol, R., Marasová, D, Moravič, M., Ozdoba, M. (2023). Forecasting blockades of conveyor transfer points based on vibrodiagnostics. *Measurement*, 216, 112884. <http://dx.doi.org/10.1016/j.measurement.2023.112884>
- Bortnowski, P., Kawalec, W., Krol, R., Ozdoba, M. (2022). Identification of conveyor belt tension with the use of its transverse vibration frequencies. *Measurement*, 190, 110706. <https://doi.org/10.1016/J.MEASUREMENT.2022.110706>
- Bortnowski, P., Król, R., Ozdoba, M. (2022). Roller damage detection method based on the measurement of transverse vibrations of the conveyor belt. *Eksploatacja i Niezawodność – Maintenance and Reliability*, 24(3). <https://doi.org/10.17531/ein.2022.3.12>
- Bortnowski, P., Nowak-Szpak, A., Król, R., Ozdoba, M. (2021). Analysis and Distribution of Conveyor Belt Noise Sources under Laboratory Conditions. *Sustainability*, 13(4). <https://doi.org/10.3390/su13042233>

- Chen, M., Ouyang, H., Li, W., Wang, D., Liu, S. (2020). Partial Frequency Assignment for Torsional Vibration Control of Complex Marine Propulsion Shafting Systems. *Appl. Sci.*, 10(147). <https://doi.org/10.3390/app10010147>
- Czech, P., Wojnar, G., Burdzik, R., Konieczny, J., Warczek, Ł. (2014). Application of the discrete wavelet transform and probabilistic neural networks in IC engine fault diagnostics. *J. Vibroengineering*, 16(4).
- Dabek, P., Szrek, J., Zimroz, R., Wodecki, J. (2022). An Automatic Procedure for Overheated Idler Detection in Belt Conveyors Using Fusion of Infrared and RGB Images Acquired during UGV Robot Inspection. *Energies*, 15(2). <https://doi.org/10.3390/en15020601>
- Damjanović, V., Jovančić, P., Aleksandrović, S. (2017). Extensive vibrations of the belt conveyor drive electromotor of a bucket wheel excavator as a result of intensified wear-and-tear of its mount support. *J. Vibroeng.*, 19(1), 214-222. <https://doi.org/10.21595/JVE.2016.17321>
- Directive 2000/14/EC of the European Parliament and of the Council of 8 May 2000 on the Approximation of the Laws of the Member States Relating to the Noise Emission in the Environment by Equipment for Use Outdoors. (2000). Council of Europe: Strasbourg, France.
- Directive 2010/75/EU of the European Parliament and of the Council of 24 November 2010 on Industrial Emissions (Integrated Pollution Prevention and Control). (2010). Council of Europe: Strasbourg, France.
- Grega, R., Krajňák, J., Moravič, M. (2018). Experimental verification of the impact of a technical gas-using pneumatic coupling on torsional oscillation. *Scientific Journal of Silesian University of Technology. Series Transport*, 99, 53-63. <https://doi.org/10.20858/sjsutst.2018.99.5>
- Guo, Y.-c., Hu, K., Wang, P.-y., Wang, Y. (2010). Dynamic simulation of belt conveyor based on virtual prototyping. *Mech. Autom. Control Eng.*, 5-7. <https://doi.org/10.1109/MACE.2010.5536884>
- Guohuan, L., Haili, Y., Shujie, L. (2011). Application of frequency converter driver in long belt conveyor. *Adv. Mater. Res.*, 340, 19-22. <https://doi.org/10.4028/www.scientific.net/AMR.340.19>
- Harrison, A. (1986). Determination of the natural frequencies of transverse vibration for conveyor belts with orthotropic properties. *J. Sound Vib.*, 110(3), 483-493. [https://doi.org/10.1016/S0022-460X\(86\)80149-3](https://doi.org/10.1016/S0022-460X(86)80149-3)
- Homišin, J., Moravič, M. (2016). Basic Conditions of the Implementation of Extremal Regulation. *The Latest Methods of Construction Design*, 325-330. https://doi.org/10.1007/978-3-319-22762-7_48
- Hou, Y., Meng, Q. (2008). Dynamic characteristics of conveyor belts. *J. China Univ. Min. Technol.*, 18(4), 629-633. [https://doi.org/10.1016/S1006-1266\(08\)60307-7](https://doi.org/10.1016/S1006-1266(08)60307-7)
- Jia, Z., Liu, Z., Vong, C.-M., Pecht, M. (2019). A rotating machinery fault diagnosis method based on feature learning of thermal images. *IEEE Access*, 7, 12348-12359. <https://doi.org/10.1109/ACCESS.2019.2893331>
- Klimenda, F., Soukup, J., Rychlikova, L., Skocilas, J. (2022). Transverse Wave Propagation in a Thin Isotropic Plate Part I. *Appl. Sci.*, 12(5). <https://doi.org/10.3390/app12052493>
- Ladányi, G. (2016). Study on the noise emission of belt conveyor idler rolls. *Annals of the University of Petroșani. Mechanical Engineering*, 18, 83-92.
- Łazarz, B., Wojnar, G. Czech, P. (2011). Early fault detection of toothed gear in exploitation conditions, *Eksploatacja i Niezawodność – Maintenance and Reliability*, 49(1), 68-77.
- Li, W., Wang, Z., Zhu, Z., Zhou, G., Chen, G. (2013). Design of Online Monitoring and Fault Diagnosis System for Belt Conveyors Based on Wavelet Packet Decomposition and Support Vector Machine. *Advances in Mechanical Engineering*, 5. <https://doi.org/10.1155/2013/797183>
- Liu, X., Pei, D., Lodewijks, G., Zhao, Z., Mei, J. (2020). Acoustic signal based fault detection on belt conveyor idlers using machine learning. *Adv. Powder Technol.*, 31(7), 2689-2698. <https://doi.org/10.1016/j.apt.2020.04.034>
- Moravič, M. (2017). Príspevok k redukcii počtu stupňov voľnosti modelu mechanickej sústavy metódou parciálnych frekvencií. *Novus Scientia 2017*. Košice: Technická univerzita v Košiciach, 123-126. (In Slovak)
- Nawrocki, W., Stryjski, R., Kostrzewski, M., Wozniak, W., Jachowicz, T. (2023). Application of the vibro-acoustic signal to evaluate wear in the spindle bearings of machining centres. In-service diagnostics in the automotive industry. *Journal of Manufacturing Processes*, 92, 165-178. <https://doi.org/10.1016/j.jmapro.2023.02.036>
- Novotný, V., Sysel, P., Prokes, A., Hanák, P., Slavicek, K., Prinosil, J. (2021). Fiber Optic Based Distributed Mechanical Vibration Sensing. *Sensors*, 21(14). <https://doi.org/10.3390/s21144779>
- Nowakowski, T., Komorski, P. (2022). Diagnostics of the drive shaft bearing based on vibrations in the high-frequency range as a part of the vehicle's self-diagnostic system. *Eksploatacja i Niezawodność – Maintenance and Reliability*, 24(1), 70-79. <http://dx.doi.org/10.17531/ein.2022.1.9>
- Ojha, S., Sarangi, D., Pal, B.K., Biswal B.B. (2014). Performance Monitoring of Vibration in Belt Conveyor System. *Journal of Engineering Research and Applications*, 4(7), 22-31.
- Pang, Y., Lodewijks, G. (2013). Pipe belt conveyor statics-comparison of simulation results and measurements. *Bulk Solids Handling*, 33(2), 52-56.

- Pišosová, M., Andejiová, M., Liptai, P., Lumnitzer, E. (2018). Objective and subjective evaluation of the risk physical factors near to conveyor system. *Adv. Sci. Technol. Res. J.*, 12(3), 188-196. <https://doi.org/10.12913/22998624/94964>
- Pytlík A, Trela K. (2016). Research on tightness loss of belt conveyor's idlers and its impact on the temperature increase of the bearing assemblies. *Journal of Sustainable Mining*, 15(2), 57-65. <https://doi.org/10.1016/j.jsm.2016.07.001>
- Rivin, E.I. (1966). *Dinamika Privoda Stankov; Mašinostrojenije*; Moskva, Russia. (In Russian)
- Qurthobi, A., Maskeliunas, R., Damaševičius, R. (2022). Detection of Mechanical Failures in Industrial Machines Using Overlapping Acoustic Anomalies: A Systematic Literature Review. *Sensors*, 22(10). <https://doi.org/10.3390/s22103888>
- Skoczylas, A., Stefaniak, P., Anufriev, S., Jachnik, B. (2021). Belt Conveyors Rollers Diagnostics Based on Acoustic Signal Collected Using Autonomous Legged Inspection Robot. *Appl. Sci.*, 11(5). <https://doi.org/10.3390/app11052299>
- Szurgacz, D., Zhironkin, S., Vöth, S., Pokorný, J., Spearing, A., Cehlár, M., Stempniak, M., Sobik, L. (2021) Thermal imaging study to determine the operational condition of a conveyor belt drive system structure. *Energies*, 14 (11). <https://doi.org/10.3390/en14113258>
- Thai, T., Kučera, P., Bernatik, A. (2021). Noise Pollution and Its Correlations with Occupational Noise-Induced Hearing Loss in Cement Plants in Vietnam. *International Journal of Environmental Research and Public Health*, 18(8). <https://doi.org/10.3390/ijerph18084229>
- Ullmann, A. Dayan, A. (1998). Exhaust volume model for dust emission control of belt conveyor transfer points. *Powder Technol.*, 96(2), 139-147.
- Utěkal, P. (1973). Aplikace metody parciálních frekvencí na zjednodušení torsních soustav hnacích soustrojí lokomotiv. *Tech. Zprávy ČKD*, 2. (In Czech)
- Wijaya, H., Rajeev, P., Gad, E., Vivekanantham, R. (2022). Automatic fault detection system for mining conveyor using distributed acoustic sensor. *Measurement*, 187, 110330. <https://doi.org/10.1016/j.measurement.2021.110330>
- Yan, C., He, X. (2010). Model and dynamic simulation of belt conveyor. *Int. Conf. Intell. Syst. Des. Eng. Appl.*, 949-951. <https://doi.org/10.1109/ISDEA.2010.331>
- Yang, M., Zhou, W., Song, T. (2020). Audio-based fault diagnosis for belt conveyor rollers. *Neurocomputing*, 397, 447-456. <https://doi.org/10.1016/j.neucom.2019.09.109>
- Yu, G., Yan, G., Ma, B., (2022). Feature enhancement method of rolling bearing acoustic signal based on RLS-RSSD. *Measurement*, 192, 110883. <https://doi.org/10.1016/j.measurement.2022.110883>
- Zeng, F., Yan, C., Wu, Q., Wang, T. (2020). Dynamic Behaviour of a Conveyor Belt Considering Non-Uniform Bulk Material Distribution for Speed Control. *Appl. Sci.*, 10(13). <https://doi.org/10.3390/app10134436>
- Zhang, Y., Li, S., Li, A., Zhang, G., Wu, M. (2023). Fault diagnosis method of belt conveyor idler based on sound signal. *J. of Mechanical Science and Technology*, 37, 69-79. <https://doi.org/10.1007/s12206-022-1208-1>
- Živanić, D., Ilanković, N., Zuber, N., Đokić, R., Zdravković, N., Zelić, A. (2021). The analysis of influential parameters on calibration and feeding accuracy of belt feeders. *Eksploatacja i Niezawodność – Maintenance and Reliability*, 23(3), 413-421. <https://doi.org/10.17531/ein.2021.3.2>